Available online at www.sciencedirect.com

ScienceDirect

Geochimica et Cosmochimica Acta 162 (2015) 83–98

Geochimica et Cosmochimica Acta

www.elsevier.com/locate/gca

Impact of iron chelators on short-term dissolution of basaltic glass

Anne Perez [a,*], Stéphanie Rossano [a,*], Nicolas Trcera [b], Aurélie Verney-Carron [c], David Huguenot [a], Eric D. van Hullebusch [a], Gilles Catillon [a], Angelina Razafitianamaharavo [d], François Guyot [e]

[a] *Université Paris-Est, Laboratoire Géomatériaux et Environnement (EA 4508), UPEM, 77454 Marne-la-Vallée, France*
[b] *Lucia Beamline, Synchrotron SOLEIL, 91192 Gif-sur-Yvette, France*
[c] *Laboratoire Interuniversitaire des Systèmes Atmosphériques, UMR-CNRS 7583, Université Paris Est Créteil, France*
[d] *Laboratoire Interdisciplinaire des Environnements Continentaux, CNRS UMR7360, Université de Lorraine, 54501 Vandoeuvre-lès-Nancy, France*
[e] *Institut de Minéralogie, de Physique des Matériaux et de Cosmochimie, Muséum National d'Histoire Naturelle, CNRS, UPMC, IRD, 75005 Paris, France*

Received 15 July 2014; accepted in revised form 14 April 2015; Available online 23 April 2015

Abstract

Although microorganisms seem to play an important role in the alteration processes of basaltic glasses in solution, the elementary mechanisms involved remain unclear in particular with regard to the role of organic ligands excreted by the cells. Two glasses, one with Fe and one without Fe were synthesized to model basaltic glass compositions. Fe in the glass was mostly Fe(III) for enhancing interaction with siderophores, yet with small but significant amounts of Fe(II) (between 10% and 30% of iron). The prepared samples were submitted to abiotic alteration experiments in buffered (pH 6.4) diluted solutions of metal-specific ligands, namely oxalic acid (OA, 10 mM), desferrioxamine (DFA, 1 mM) or 2,2′-bipyridyl (BPI, 1 mM). Element release from the glass into the solution after short term alteration (maximum 1 week) was measured by ICP-OES, and normalized mass losses and relative release ratios (with respect to Si) were evaluated for each element in each experimental condition. The presence of organic ligands had a significant effect on the dissolution of both glasses. Trivalent metals chelators (OA, DFA) impacted on the release of Fe^{3+} and Al^{3+}, and thus on the global dissolution of both glasses, enhancing all release rates and dissolution stoichiometry (release rates were increased up to 7 times for Al or Fe). As expected, the mostly divalent metal chelator BPI interacted preferentially with Ca^{2+}, Mg^{2+} and Fe^{2+}. This study thus allows to highlight the central roles of iron and aluminium in interaction with some organic ligands in the alteration processes of basaltic glasses. It thus provides a step toward understanding the biological contribution of this fundamental geological process.

1. INTRODUCTION

Alteration mechanisms of glasses constitute a major area of interest in many research fields. In an environmental context, studies about nuclear glass weathering have been largely reported in the literature. Short-term alteration experiments have been designed to determine initial dissolution rates (Luckscheiter and Nesovic, 2004; Fournier et al., 2014) while residual dissolution rates have been calculated for very long-term alteration experiments (Curti et al., 2006; Libourel et al., 2011; Gin et al., 2012, 2013, 2014). These short and long-term dissolution kinetics were investigated with respect to parameters such as temperature and pH (Pierce et al., 2008) and glass elemental composition

* Corresponding authors at: Laboratoire Géomatériaux & Environnement, 5 boulevard Descartes, 77 420 Champs-sur-Marne, France.
E-mail addresses: anne.perez@u-pem.fr (A. Perez), stephanie.rossano@u-pem.fr (S. Rossano).

http://dx.doi.org/10.1016/j.gca.2015.04.025
0016-7037/

(Gin et al., 2012), and they have been coupled to studies of the alteration gel (Rebiscoul et al., 2005; Jollivet et al., 2008; Gin et al., 2015; Hellmann et al., 2015) or of secondary phases (Pelegrin et al., 2010). These experiments were performed in pure water, water enriched in elements from the glass (Luckscheiter and Nesovic, 2004; Thien et al., 2012) and in salt solutions (Godon et al., 1988; Abdelouas et al., 1993). The stability and dissolution behavior of bioglass, designed to form chemical bonds with living tissues (Souza et al., 2013), is of interest to the medical field. Glass alteration is also a crucial issue in the field of cultural heritage, especially with respect to the restoration and conservation of stained glass windows (see, for example Silvestri et al., 2005; Warkinson et al., 2005; Cagno et al., 2011; Gentaz, 2011; Schalm et al., 2010; Sterpenich, 2011; Lombardo et al., 2013). Finally, in a geological context, igneous rock alteration processes and especially basaltic glass-fluid interactions have been examined, as they provide knowledge about the major biogeochemical cycles of the Earth (Fliegel et al., 2012; Knowles et al., 2013). For example, glass weathering plays a central role in geological sequestration of CO_2 (Knauss et al., 2005) and contributes to the cycling of elements such as calcium, magnesium, silicon, iron and also oxygen in soils, rivers, lakes and oceans (Gislason et al., 2009). Basaltic glasses are also considered to be analogues of some nuclear glasses (Crovisier et al., 2003; Parruzot et al., 2015) and by extension, of archaeological glasses (Verney-Carron et al., 2008; Michelin et al., 2013).

The dissolution mechanisms of silicate glasses in solution have been extensively documented in the literature (Techer et al., 2000; Oelkers, 2001; Stroncik and Schmincke, 2002; Crovisier et al., 2003; Verney-Carron et al., 2008; Fournier et al., 2014). However, few studies have investigated this alteration under the action of microorganisms (Drewello and Weissmann, 1997; Gorbushina and Palinska, 1999; Gallien et al., 2001; Aouad et al., 2006; Stockmann et al., 2012; Shen et al., 2014) despite their well known interaction with mineral surfaces in general (Hutchens, 2009). Microorganisms have been shown to either enhance or inhibit dissolution of most minerals by a variety of mechanisms, especially through a direct impact of bacteria attached to the glass surface (Hutchens, 2009) and also by considering the possible effect of microbial metabolites excreted by the cells (Ullman et al., 1996). An example of this is siderophores, which are excreted in response to iron deficiency by different biological sources such as bacteria or fungi, in soils and in oceans. They have been shown to target and acquire specifically iron from iron-containing minerals and to mediate metal transport and re-absorption into the cell (Kalinowski et al., 2000b; Kraemer, 2004; Wolff Boenish and Traina, 2007). As a consequence, they have been described as catalytic agents of the dissolution of those minerals. A considerable number of studies have described this ligand-controlled dissolution as a surface controlled process to which an empirical rate law can be applied:

$$R_t = R_H + R_L \quad (1)$$

where R_t is the overall dissolution rate, R_H the proton-promoted rate and R_L a ligand-promoted term (Furrer and Stumm, 1986; Welch and Ullmann, 1993; Drever and Stillings, 1997; Stillings et al., 1998; Rosenberg and Maurice, 2003; Cama and Ganor, 2006).

Iron is a micronutrient that is essential for a range of crucial enzymatic processes in most organisms. In most environments iron deficiency is triggered by low iron bioavailability. To overcome this limitation, microorganisms and especially bacteria are known to sequester iron using organic molecules (Kraemer, 2004). Most siderophores are Fe^{3+}-ligands, but they are most of the time able to bind ions other than Fe^{3+} and notably divalent cations (Hernlem et al., 1996; Braud et al., 2009; Brandel et al., 2012). Although considerable research has been carried out to examine the processes and products of abiotic basaltic glass weathering, little work has been done to quantitatively understand their weathering process in the presence of bacteria and organic bioproducts (Staudigel, 1995).

In this work, the impact of siderophores on the alteration of two synthetic basaltic glasses was investigated as a first step towards the understanding of natural systems. Three iron chelators, namely oxalic acid (OA), desferrioxamine (DFA) and 2,2′-bipyridyl (BPI) were chosen on the basis of their respective affinity with iron in its Fe(II) and/or Fe(III) oxidation states. The effect of OA on mineral dissolution has been reported in the literature (Furrer and Stumm, 1986; Zinder et al., 1986; Welch and Ullman, 1992; Stillings et al., 1995; Drever and Stillings, 1997; Oelkers and Gislason, 2001; Cheah et al., 2003; Wang et al., 2005; Olsen and Rimstidt, 2008; Martinez-Luevanos et al., 2011). OA can be complexed with both ferric and ferrous ions but its affinity with trivalent metal cations is stronger. DFA is an hexadendate siderophore produced by the soil bacterial strain *Streptomyces pilosus,* in which three hydroxamate groups, each acting as a bidentate ligand, contribute to the specific ligation of Fe^{3+} and therefore to the formation of very stable 1:1 complexes with aqueous Fe(III) (Kraemer et al., 1999; Liermann et al., 2000; Elandalloussi, 2003). By contrast, BPI is a bidendate chelator that predominantly binds aqueous Fe(II). Three molecules of BPI are necessary to coordinate with one Fe atom. While the impact of DFA on dissolution of mineral phases has been widely investigated in studies which illustrate the synergistic effect that the molecule has on dissolution (Watteau and Berthelin, 1994; Kraemer et al., 1999; Liermann et al., 2000; Cocozza et al., 2001; Cheah et al., 2003; Wolff-Boenisch, 2007), the interactions between 2,2′-bipyridyl and minerals have been the goal of only a few studies mainly focusing on the adsorption process of BPI on solids surfaces (Coluccia et al., 1978; Ferreiro et al., 1983).

The use of Fe-specific chelators implies that we are focussing on the solvation of Fe and its possible impact on the global dissolution of the glass. In this regard, two different glasses (with and without Fe) were prepared using a simplified basaltic glass composition. Experiments were performed to evaluate the significance of the ligand-promoted dissolution and to determine the effect of three organic ligands, namely OA, DFA and BPI, on basaltic glass dissolution mechanisms at pH 6.4 and 25 °C. Experimental conditions were chosen to ensure a negligible

effect of proton-promoted dissolution. Siderophore concentrations were deliberately chosen to be higher than the concentrations usually found in nature, in order to mimic localized microenvironments found at the interfacial region between bacteria and silicate materials. Their respective values were chosen on the base of mineral dissolution studies involving OA (Stillings et al., 1995; Cheah et al., 2003) and DFA (Hersman et al., 1995). Oxalic acid concentrations were chosen to be higher than those of the other iron chelators considering the relative abundance of organic acids in natural environment with respect to siderophores.

2. MATERIAL AND METHODS

2.1. Glass materials

Two glass compositions were studied (Table 1). The first was prepared according to a simplified typical Mid Oceanic Ridge Basalt (MORB) composition (GERM, 2000) and the second (HAPLO) is an iron-free glass of close composition except that iron has been replaced by magnesium.

Samples were prepared from powdered oxides and carbonates (SiO_2, Al_2O_3, Fe_2O_3, $CaCO_3$, $MgCO_3$, Na_2CO_3, TiO_2, K_2CO_3). The starting materials were dried overnight at 100 °C, weighed, mixed in an agate mortar, and placed in a platinum crucible. Glass preparation took place in a high-temperature furnace Carbolite HTF 1700. To start the decarbonation of the mixture, the temperature was maintained at 600 °C for 45 min. Then the temperature was increased up to 1500 °C and kept for 1 h to homogenize the melt. The bottom of the crucible was then poured into water to quench the silicate melt into a glass. The resulting glass was then coarsely ground and placed into the crucible. The temperature was increased up to 1630 °C and maintained for 1 h in order to pour the melted glass in a graphite cylindrical crucible at ambient temperature. The cylindrical piece of glass obtained was annealed overnight at 600 °C. This temperature was chosen according to Differential Scanning Calorimetry measurements performed on a SETARAM labSys EVO-1600 (temperature range 30–1550 °C, increase in temperature of 10 °C.min^{-1} under reconstituted air). Glass-transition temperatures were equal to 676 °C and 735 °C for MORB and HAPLO glasses, respectively. The prepared glasses were then ground into powder and the 100–200 μm size fraction was selected. This fraction was cleaned using washing by sedimentation in acetone to remove fine particles and then sterilized for 10–15 min at 200 °C.

Table 1
Nominal composition of samples.

	MORB (wt.%)	HAPLO (wt.%)
SiO_2	48.6	51.6
Al_2O_3	15.7	16.7
FeO	12.5	0.0
CaO	11.1	11.8
MgO	7.7	15.2
Na_2O	2.7	2.9
TiO_2	1.4	1.5
K_2O	0.2	0.3

X-ray Diffraction (XRD) confirmed that the synthesized solids were purely amorphous. The XRD data were collected from 2.5 to 120° 2θ using a Brucker D8 XRD diffractometer. X-ray absorption at the Fe K-edge was used to confirm that iron oxidation state was not changing between the different steps of sample preparation (before and after annealing, before and after sterilization). Measurements were performed on the LUCIA beamline (SOLEIL synchrotron). All the spectra were similar implying that the redox ratio did not vary during processing. The obtained spectra were characteristic of a glass mainly containing Fe(III). Fe(II) content can be estimated to 10 to 30 at.% of total iron.

The specific surface area of the samples was measured on 5.3 g of glass powder (100–200 μm size fraction) using nitrogen adsorption and application of the Brunauer-Emmett-Teller (BET) method (Brunauer et al., 1938). Measured values are 0.040 ± 0.0 m^2/g for the MORB and 0.038 ± 0.01 m^2/g for the HAPLO glass. For comparison, the geometric surface was evaluated to 0.16 m^2/g considering that the powder was made of spheres whose diameter ranged between 100 and 200 μm.

2.2. Dissolution experiments

Dissolution experiments were performed in highly diluted conditions to prevent saturation effects and back-reactions on the dissolution rates. For the experiments, splits of basaltic glass (0.1 g) were immersed in 40 mL of liquid medium contained within 50 mL sterile polypropylene flasks. The calculated surface to volume (S/V) ratios are 100 m^{-1} and 95 m^{-1} for the MORB and HAPLO samples, respectively. To assess the reproducibility of the results, two sets of experiments (from glass synthesis to alteration) were successively performed.

The liquid medium was prepared with 1 L of Ultrapure water (UPW) (Electrical Resistivity 18.2 MΩ) mixed with 1 mM $NaHCO_3$ pH buffer and 30.8 μL HNO_3 65% in order to maintain a pH of 6.4. Aliquots were measured from each tube after the experiments with an Ag/AgCl type electrode to control the stability of the pH, and the remainder of each sample was kept for analysis. OA, DFA (*Alfa Aesar*) or BPI (*Alfa Aesar*) were added to achieve initial concentrations of 10 mM for OA, 1 mM for DFA and BPI, respectively. The OA solution was prepared by mixing 0.1 L solution of 100 mM OA with 0.80 g of NaOH in order to maintain a pH of 6.4. The solution was then diluted 10 times with UPW and mixed with 1 mM $NaHCO_3$ and 30.8 μL HNO_3 65% to maintain this pH during experiments. Controls without organic molecules added, labeled UPW, were also monitored. The suspensions were continuously shaken on an agitation table at 160 rpm and 25 °C for durations ranging from 8 h to 7 days.

Sampling was performed after 0.3, 1, 2, 4, 7 days for the UPW and OA solutions and after 0.3, 1, 2, 2.8, 5, 7 days for the DFA and BPI solutions respectively, by filtering the content of each flask with 0.2 μm cellulose-acetate syringe filters.

Table 2
Concentrations (in μg/L) of elements released from the MORB glass into oxalic acid (OA), desferrioxamine (DFA), 2,2′-bipyridyl (BPI) and ultrapure water (UPW) solutions. Sample time varies between 8 h (H) to 7 d (D). (1) and (2) correspond to both sets of experiments. Standard deviations correspond to analytical absolute errors on concentrations for a specific area of 0.04 g/m^2.

	Sample time	Si		Al		Fe		Ca		Mg	
		(1)	(2)	(1)	(2)	(1)	(2)	(1)	(2)	(1)	(2)
OA	8H	26.1 ± 2.6	32.2 ± 2.6	13.6 ± 0.3	17.5 ± 0.3	36.2 ± 3.0	42.3 ± 3.0	22.5 ± 8.0	25.7 ± 8.0	35.9 ± 3.6	25.5 ± 3.6
	1D	82.0 ± 1.2	92.2 ± 1.2	31.5 ± 0.3	29.2 ± 0.3	52.5 ± 0.9	57.9 ± 0.9	41.5 ± 8.0	49.9 ± 8.0	44.7 ± 3.6	42.0 ± 3.6
	2D	120.1 ± 1.7	84.5 ± 1.2	63.4 ± 1.0	21.1 ± 0.3	88.7 ± 0.9	43.9 ± 0.9	88.1 ± 10.7	64.9 ± 10.7	53.6 ± 2.3	40.3 ± 3.6
	3D	158.1 ± 1.7	155.8 ± 1.7	56.3 ± 1.0	59.6 ± 2.5	70.9 ± 0.9	81.3 ± 0.9	62.6 ± 10.7	53.5 ± 10.7	57.4 ± 2.3	62.6 ± 2.3
	4D	179.4 ± 1.7	191.7 ± 1.7	73.6 ± 1.0	72.4 ± 1.0	92.1 ± 0.9	104.1 ± 0.9	33.0 ± 8.0	36.7 ± 8.0	63.3 ± 2.3	72.5 ± 2.3
	7D	351.0 ± 1.7	292.6 ± 2.0	150.0 ± 1.8	106.2 ± 1.0	152.1 ± 0.9	141.6 ± 0.9	49.4 ± 8.0	48.1 ± 8.4	104.5 ± 3.6	97.6 ± 2.3
DFA	8H	29.1 ± 2.6	32.9 ± 2.6	2.7 ± 0.3	10.9 ± 0.3	29.8 ± 3.0	28.1 ± 3.0	46.2 ± 8.0	57.0 ± 10.7	34.9 ± 3.6	37.0 ± 3.6
	1D	54.2 ± 1.2	59.1 ± 1.2	27.3 ± 0.3	32.3 ± 0.3	58.2 ± 0.9	57.1 ± 0.9	75.5 ± 10.7	105.4 ± 8.2	49.4 ± 3.6	52.3 ± 2.3
	2D	97.9 ± 1.2	68.6 ± 1.2	55.6 ± 1.0	45.5 ± 0.3	90.8 ± 0.9	110.2 ± 0.9	116.5 ± 8.2	108.5 ± 8.2	70.2 ± 2.3	60.0 ± 2.3
	2.7D	143.4 ± 1.7	132.0 ± 1.7	70.0 ± 1.0	67.6 ± 1.0	109.8 ± 0.9	107.0 ± 0.9	136.8 ± 8.2	133.2 ± 8.2	78.7 ± 2.3	81.0 ± 2.3
	5D	245.6 ± 2.0	203.3 ± 2.0	110.7 ± 1.8	96.3 ± 1.0	152.2 ± 0.9	153.3 ± 0.9	178.5 ± 8.2	224.8 ± 8.2	102.6 ± 3.6	103.3 ± 3.6
	7D	296.5 ± 2.0	315.3 ± 1.7	125.7 ± 1.8	139.0 ± 1.8	182.1 ± 0.9	200.9 ± 2.0	206.4 ± 8.2	263.0 ± 8.2	113.5 ± 3.6	136.1 ± 3.6
BPI	8H	37.7 ± 2.6	26.8 ± 2.6	0.3 ± 0.3	0.4 ± 0.3	10.1 ± 3.0	4.7 ± 3.0	45.6 ± 8.0	24.0 ± 8.0	47.7 ± 3.6	41.7 ± 3.6
	1D	50.9 ± 1.2	68.4 ± 1.2	0.0 ± 0.3	7.8 ± 0.3	12.5 ± 3.0	7.9 ± 3.0	71.6 ± 10.7	90.4 ± 10.7	58.6 ± 2.3	65.1 ± 2.3
	2D	93.4 ± 1.2	85.7 ± 1.2	7.6 ± 0.3	8.2 ± 0.3	20.5 ± 3.0	12.6 ± 3.0	118.0 ± 8.2	125.3 ± 8.2	76.1 ± 2.3	78.5 ± 2.3
	2.7D	113.6 ± 1.7	107.0 ± 1.7	12.5 ± 0.3	10.4 ± 0.3	23.2 ± 3.0	21.4 ± 3.0	135.3 ± 8.2	151.9 ± 8.2	84.1 ± 2.3	87.9 ± 2.3
	5D	180.8 ± 1.7	150.2 ± 1.7	27.4 ± 0.3	15.2 ± 0.3	30.5 ± 3.0	40.4 ± 3.0	171.0 ± 8.2	171.8 ± 8.2	97.9 ± 2.3	96.0 ± 2.3
	7D	157.9 ± 1.7	165.6 ± 1.7	22.2 ± 0.3	12.8 ± 0.3	36.5 ± 3.0	54.4 ± 0.9	123.5 ± 8.2	190.3 ± 8.2	84.1 ± 2.3	99.5 ± 2.3
UPW	8H	9.5 ± 2.6	2.3 ± 2.6	1.3 ± 0.3	0.08 ± 0.3	0.0	0.0	20.2 ± 8.0	21.6 ± 8.0	19.6 ± 3.6	21.3 ± 3.6
	1D	23.2 ± 2.6	39.3 ± 2.6	0.9 ± 0.3	1.4 ± 0.3	0.0	0.0	36.6 ± 8.0	32.4 ± 8.0	23.9 ± 3.6	29.6 ± 3.6
	2D	35.7 ± 2.6	50.7 ± 1.2	3.2 ± 0.3	1.9 ± 0.3	0.0	0.0	55.9 ± 10.7	58.7 ± 10.7	28.2 ± 3.6	26.2 ± 3.6
	3D	54.5 ± 1.2	81.6 ± 1.2	19.2 ± 0.3	29.8 ± 0.3	0.0	0.0	46.6 ± 8.0	78.5 ± 10.7	31.8 ± 3.6	32.5 ± 3.6
	4D	66.3 ± 1.2	73.8 ± 1.2	8.6 ± 0.3	27.0 ± 0.3	0.0	0.0	65.6 ± 10.7	62.9 ± 10.7	34.9 ± 3.6	34.0 ± 3.6
	7D	84.7 ± 1.2	102.9 ± 1.7	29.2 ± 0.3	37.6 ± 0.3	0.0	0.0	75.8 ± 10.7	77.6 ± 10.7	32.5 ± 3.6	41.8 ± 3.6

The amounts of dissolved Si, Al, Fe, Ca and Mg in each sample were analyzed using a Perkin Elmer Optima 8300 ion coupled plasma optical emission spectrometer (ICP-OES). Ti and *K* concentrations in solution were not analyzed because of their low concentration in the solid. Na was also exempted from ICP-OES analysis because it was present in the buffer solution at a concentration of 1 mM. Si, Al, Fe, Ca and Mg ICP standard solutions were prepared by dissolving a commercial multielement solution (*Merck Chemicals*) in UPW. Both alteration solutions and standards were acidified with 1% HNO_3 prior to analysis. Each analysis consisted in the average of three successive measurements.

For each element i and at each dissolution time, the normalized mass loss NL_i from the glass into the solution was calculated using Eq. (2). Considering a linear regression, the initial slope of the curve was calculated in order to evaluate the initial rate of dissolution r_i as given in Eq. (3):

$$NL_i = \frac{[i]}{S/V \times x_i} \tag{2}$$

$$r_i = \frac{dNL_i}{dt} = \frac{d[i]}{S/V \times x_i \times dt} \tag{3}$$

where $[i]$ is the concentration ($mg.L^{-1}$) of the element i in solution, S the surface of the glass powder in contact with the fluid, V the volume of solution and x_i the mass percentage of the element i in the glass. The variations of V and S were considered as negligible and were not taken into account in the calculations.

Dissolution stoichiometry was assessed by the use of the Relative Release Ratio that quantifies the relative release of one element X from the glass with respect to Si (Holdren and Spyer, 1985):

$$RRR_{X/Si} = \frac{(X/Si)_{solution}}{(X/Si)_{solid}} \tag{4}$$

When $RRR_{X/Si} = 1$, dissolution is stoichiometric for each element X relative to Si. When $RRR_{X/Si}$ is greater than 1, element X is preferentially released with respect to Si; in contrast at values lower than 1 Si is released preferentially to element X.

2.3. Uncertainty calculations

Experimental specific surface measurements depend on the quantity of the sample, which is determined by the experimental device. Due to the granulometry of the powders (100–200 μm), measured specific surface areas are small. In consequence the absolute error on the specific area value is high and will not be taken into account for the representation of the error bars on the graphs.

For a specific surface area value ($0.04\ m^2\ g^{-1}$ in this work), analytical absolute errors on elemental concentrations were determined for each element (Si, Al, Fe, Ca, Mg) by analyzing several dilutions (10 ppb, 50 ppb, 100 ppb, 200 ppb, 500 ppb and 1 ppm) of a multielement solution. Five measurements were performed for each dilution and each element and dispersion was evaluated for a certain range of concentration by calculating the standard deviation (SD). The analytical absolute error on concentrations was considered as ±2SD to ensure a confidence interval of 96%.

For a given specific surface, and considering the variations of V and glass composition as negligible, the relative errors on NL are thus equal to relative errors on concentrations.

3. RESULTS

Basaltic glass dissolution kinetics were monitored at $pH = pK_A(H_2CO_3/HCO_3^-) = 6.4$ to minimize proton promoted dissolution and to enhance the effect of organic ligands (Welch and Ullman, 1992; Furrer and Stumm, 1986). No relevant change in pH occurred in the UPW, OA or DFA solutions and pH values all ranged between 6.40 and 6.83. The pH monitoring of BPI solutions gave values ranging from 7.02 to 7.28.

The concentrations of the elements released from the MORB and HAPLO glasses into the solution are given in the Tables 2 and 3, respectively, for both sets of experiments.

Si concentrations (<1 mg/L) in all solutions after 7 d of the experiments are much lower than the calculated concentration of Si in a solution in equilibrium with amorphous silica (54 mg/L) or quartz (5 mg/L) (Gunnarson and Arnorsson, 2000). This attests to the far-from-equilibrium conditions of the dissolution reaction despite the rate model considered (Grambow, 1985; Daux et al., 1997; Oelkers and Gislason, 2001). However, affinity effects on the release rate cannot completely be excluded in such experiments (S. Gin, personnal communication).

3.1. Normalized mass loss profiles

Normalized mass losses (NLs) for Si, Al, Fe, Ca and Mg during alteration experiments in the UPW, OA, DFA and BPI solutions are plotted as a function of time in Fig. 1 for the MORB composition and in Fig. 2 for the HAPLO composition.

In most cases, NL values increase with time whatever the cation, the organic ligand and the glass composition considered. The increase appears to be linear during the first 2–3 d indicating a constant rate of dissolution. NL profiles are similar for MORB and HAPLO glasses.

For each element, the highest NL after 7 d of dissolution are systematically observed in the OA and DFA dissolution profiles. In the DFA solution, a progressive decrease in slopes is observed. When dissolution occurs in the presence of oxalate, a discontinuity is noticed on Al and Fe mass loss profiles after 2 d (MORB duplicates set 1, HAPLO duplicates set 1), 1 d (MORB duplicates set 2) and 3 d (HAPLO duplicates set 2). Despite these changes of slope, NL values continue to increase until the end of the dissolution experiments. These discontinuities in Al and Fe NLs may be due to local precipitation of secondary mineral phases. As alteration layers are very thin (ranging from a few tens to a few hundred angstroms, according to calculations made on the basis of the solution chemistry) such secondary phases would not be detected by Scanning Electron Microscopy (Chou and Wollast, 1984). Transmission electron microscopy on

Table 3
Concentrations (in μg/L) of elements released from the HAPLO glass into oxalic acid (OA), desferrioxamine (DFA), 2,2′-bipyridyl (BPI) and ultrapure water (UPW) solutions. Sample time varies between 8 h (H) to 7 d (D). (1) and (2) correspond to both sets of experiments. Standard deviations correspond to analytical absolute errors on concentrations for a specific area of 0.04 g/m^2.

	Sample time	Si		Al		Ca		Mg	
		(1)	(2)	(1)	(2)	(1)	(2)	(1)	(2)
OA	8H	24.1 ± 2.6	31.3 ± 2.6	22.1 ± 0.3	19.4 ± 0.3	25.3 ± 8.0	20.6 ± 8.0	61.4 ± 2.3	41.8 ± 3.6
	1D	49.7 ± 2.6	60.1 ± 1.2	41.0 ± 0.3	38.4 ± 0.3	47.1 ± 8.0	50.9 ± 10.7	85.4 ± 2.3	69.8 ± 2.3
	2D	102.5 ± 1.7	189.7 ± 1.7	68.0 ± 1.0	116.8 ± 1.8	79.2 ± 10.7	95.0 ± 10.7	125.1 ± 3.6	178.0 ± 3.6
	3D	175.4 ± 1.7	121.4 ± 1.7	107.3 ± 1.8	67.9 ± 1.0	113.1 ± 8.2	116.7 ± 8.2	164.6 ± 3.6	110.8 ± 3.6
	4D	183.6 ± 1.7	132.7 ± 1.7	96.4 ± 1.0	70.9 ± 1.0	124.8 ± 8.2	126.5 ± 8.2	158.0 ± 3.6	110.0 ± 3.6
	7D	355.0 ± 1.7	436.6 ± 1.7	179.1 ± 1.8	200.5 ± 1.8	138.9 ± 8.2	151.0 ± 8.2	240.7 ± 6.7	262.4 ± 6.7
DFA	8H	15.0 ± 2.6	19.8 ± 2.6	4.9 ± 0.3	7.9 ± 0.3	25.3 ± 8.0	11.3 ± 8.0	45.1 ± 3.6	46.2 ± 3.6
	1D	31.1 ± 2.6	31.1 ± 2.6	24.8 ± 0.3	18.7 ± 0.3	47.6 ± 8.0	57.8 ± 10.7	71.1 ± 2.3	64.0 ± 2.3
	2D	61.8 ± 1.2	52.7 ± 1.2	45.6 ± 0.3	37.9 ± 0.3	68.4 ± 10.7	62.1 ± 10.7	93.4 ± 2.3	82.2 ± 2.3
	2.7D	88.0 ± 1.2	–	57.7 ± 1.0	–	–	–	106.0 ± 3.6	–
	5D	169.8 ± 1.7	150.6 ± 1.7	87.3 ± 1.0	83.0 ± 1.0	–	126.5 ± 8.2	136.0 ± 3.6	139.2 ± 3.6
	7D	202.4 ± 1.7	169.0 ± 1.7	96.9 ± 1.0	91.0 ± 1.0	118.0 ± 8.2	123.8 ± 8.2	145.3 ± 3.6	184.5 ± 3.6
BPI	8H	17.9 ± 2.6	26.2 ± 2.6	2.2 ± 0.3	3.4 ± 0.3	21.1 ± 8.0	25.4 ± 8.0	51.8 ± 2.3	46.8 ± 3.6
	1D	28.7 ± 2.6	35.3 ± 2.6	2.7 ± 0.3	2.6 ± 0.3	33.9 ± 8.0	38.8 ± 8.0	65.5 ± 2.3	53.2 ± 2.3
	2D	46.8 ± 2.6	63.1 ± 1.2	6.7 ± 0.3	8.1 ± 0.3	46.1 ± 8.0	44.1 ± 8.0	80.2 ± 2.3	75.9 ± 2.3
	2.7D	67.3 ± 1.2	70.0 ± 1.2	15.8 ± 0.3	14.1 ± 0.3	49.3 ± 8.0	47.8 ± 8.0	88.1 ± 2.3	73.6 ± 2.3
	5D	126.6 ± 1.7	96.1 ± 1.2	38.0 ± 0.3	17.3 ± 0.3	66.6 ± 10.7	52.9 ± 10.7	106.8 ± 3.6	96.5 ± 2.3
	7D	107.8 ± 1.7	115.5 ± 1.7	23.3 ± 0.3	18.8 ± 0.3	58.7 ± 10.7	56.0 ± 10.7	102.2 ± 3.6	100.8 ± 3.6
UPW	8H	21.2 ± 2.6	11.1 ± 2.6	2.1 ± 0.3	0.1 ± 0.3	9.2 ± 8.0	10.3 ± 8.0	34.0 ± 3.6	36.6 ± 3.6
	1D	31.4 ± 2.6	34.5 ± 2.6	1.5 ± 0.3	6.9 ± 0.3	21.0 ± 8.0	25.5 ± 8.0	47.0 ± 3.6	54.0 ± 2.3
	2D	49.2 ± 2.6	49.7 ± 2.6	2.3 ± 0.3	7.12 ± 0.3	35.4 ± 8.0	47.5 ± 8.0	67.9 ± 2.3	60.3 ± 2.3
	3D	64.4 ± 1.2	68.6 ± 1.2	3.8 ± 0.3	15.3 ± 0.3	–	58.4 ± 10.7	75.9 ± 2.3	70.8 ± 2.3
	4D	88.5 ± 1.2	63.6 ± 1.2	11.4 ± 0.3	15.1 ± 0.3	–	63.3 ± 10.7	85.2 ± 2.3	80.1 ± 2.3
	7D	152.9 ± 1.7	107.4 ± 1.7	26.8 ± 0.3	28.2 ± 0.3	68.7 ± 10.7	75.5 ± 10.7	140.3 ± 3.6	134.9 ± 3.6

focused ion beam thin sections will be performed in a separate study. Similarly, in the presence of OA, the NLs(Ca) increase only during the first 2 d, then decrease. This is also characteristic of precipitation, in agreement with Welch and Ullmann (1992) who observed that oxalate could induce the formation of Ca-oxalate precipitates.

The lowest NL values for each elements are those recorded for the UPW and BPI solutions after 7 d. In the UPW solution, Fe is systematically below the detection limit (2 μg/L); this is assumed to be related either to its non-release or to its reprecipitation in insoluble phases. While a slight decrease is observed in the UPW dissolution profiles slopes after 3 or 4 d, a significant decline of element release is more clearly observed when dissolution occurs in the presence of BPI. In this case, the slope at the end of the experiment is systematically negative for the first set of MORB replicates and for the HAPLO glass.

The similarity of the results from the two sets of experiments attests to the reproducibility of the involved mechanisms. Considering the closeness of the NL values for similar conditions and time compared with the absolute error for the specific area, the data obtained for the replicate experiments are averaged from this point forward.

3.2. Initial dissolution rates

Initial dissolution rates were calculated for all glass compositions in all alteration solutions and are shown in Table 4. The Si dissolution rate of MORB glass in solution without ligands is of the same order of magnitude as that determined by Gislason and Oelkers (2003) (0.1 mg m^{-2} d^{-1}) at pH = 6.75 and 30 °C. This value is also consistent with that determined by Stockmann et al. (2012) (0.04 mg m^{-2} d^{-1}) and Galeczka et al. (2014) (0.6 mg m^{-2} d^{-1}) at pH 6.4, 25 °C and pH 6.7, 22 °C, respectively. However, it should be noted that there are significant differences between the numerous dissolution rates values of basaltic glasses reported in the literature, mainly because of the difficulties in characterizing the reactive surface area, and of the various combinations of experimental parameters (pH, temperature, solution chemistry...) (Daux et al., 1997; Techer et al., 2000; Wolff-Boenish, 2011).

NL profiles (Figs. 1 and 2) reveal similarities in between the dissolution agents. OA and DFA appear to have similar impacts on dissolution despite the glass used. BPI has a moderate impact on dissolution and is similar to that of UPW for the Al and Fe dissolution profiles. The calculation of dissolution rates values allows to slightly nuance those results, notably from one glass composition (MORB) to another (HAPLO). As a consequence, MORB and HAPLO dissolution rates are described separately and plotted in Fig. 3.

For the MORB glass, OA and DFA have comparable effects on initial dissolution rates, causing increases in the rates calculated for free-ligand solutions by at least four times. Dissolution in the presence of OA and DFA is

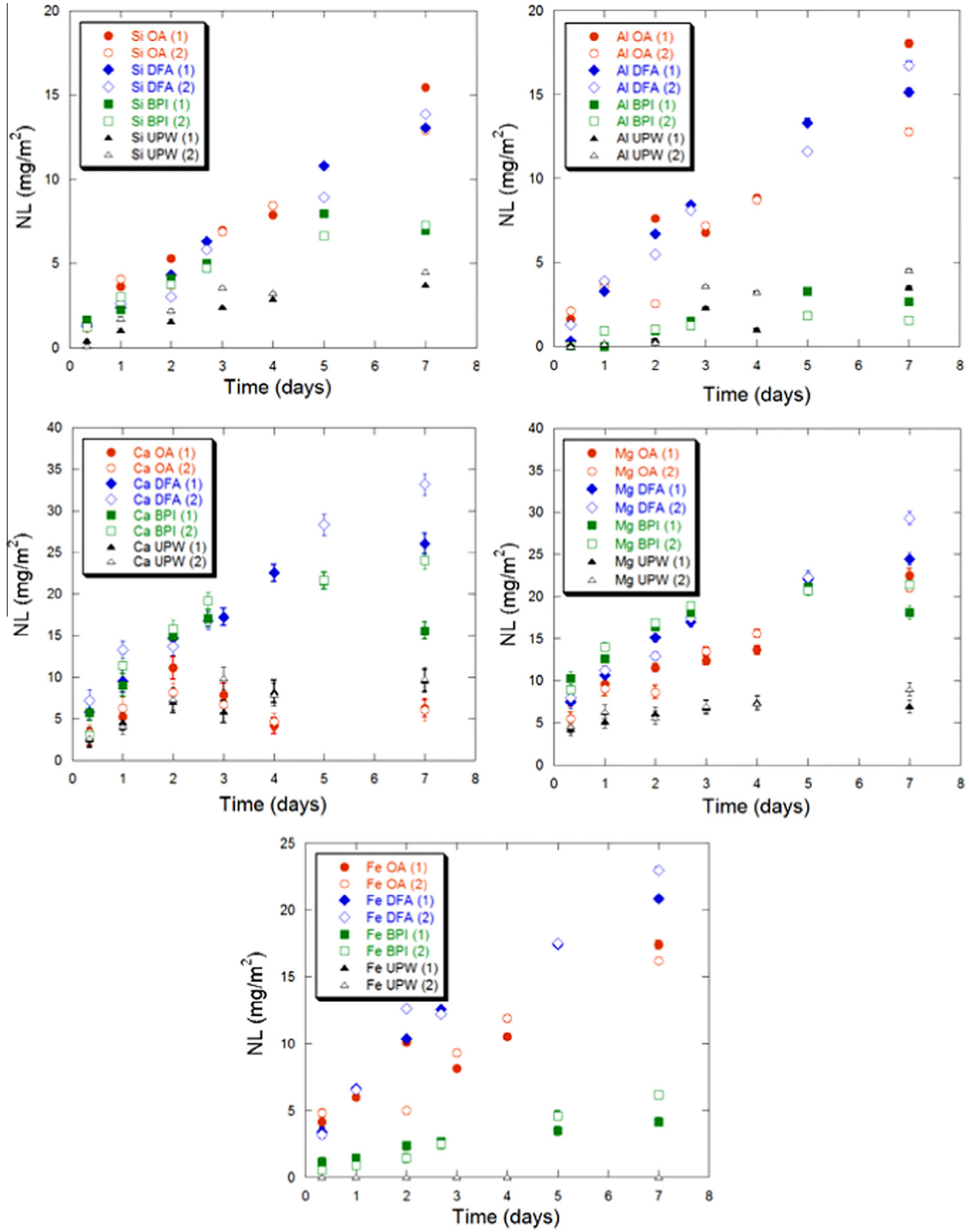

Fig. 1. Normalized mass-loss (NL) profiles of Si, Al, Ca, Mg and Fe during experiments performed on MORB glass at 25 °C and pH 6.4 in the presence of oxalic acid (OA), desferrioxamine (DFA), 2,2′-bibyridyl (BPI) or in ultrapure water (UPW) only. Full and empty symbols represent the first (1) and second (2) sets of experiments, respectively. For each NL value, the absolute error is calculated from the technical relative error in concentration.

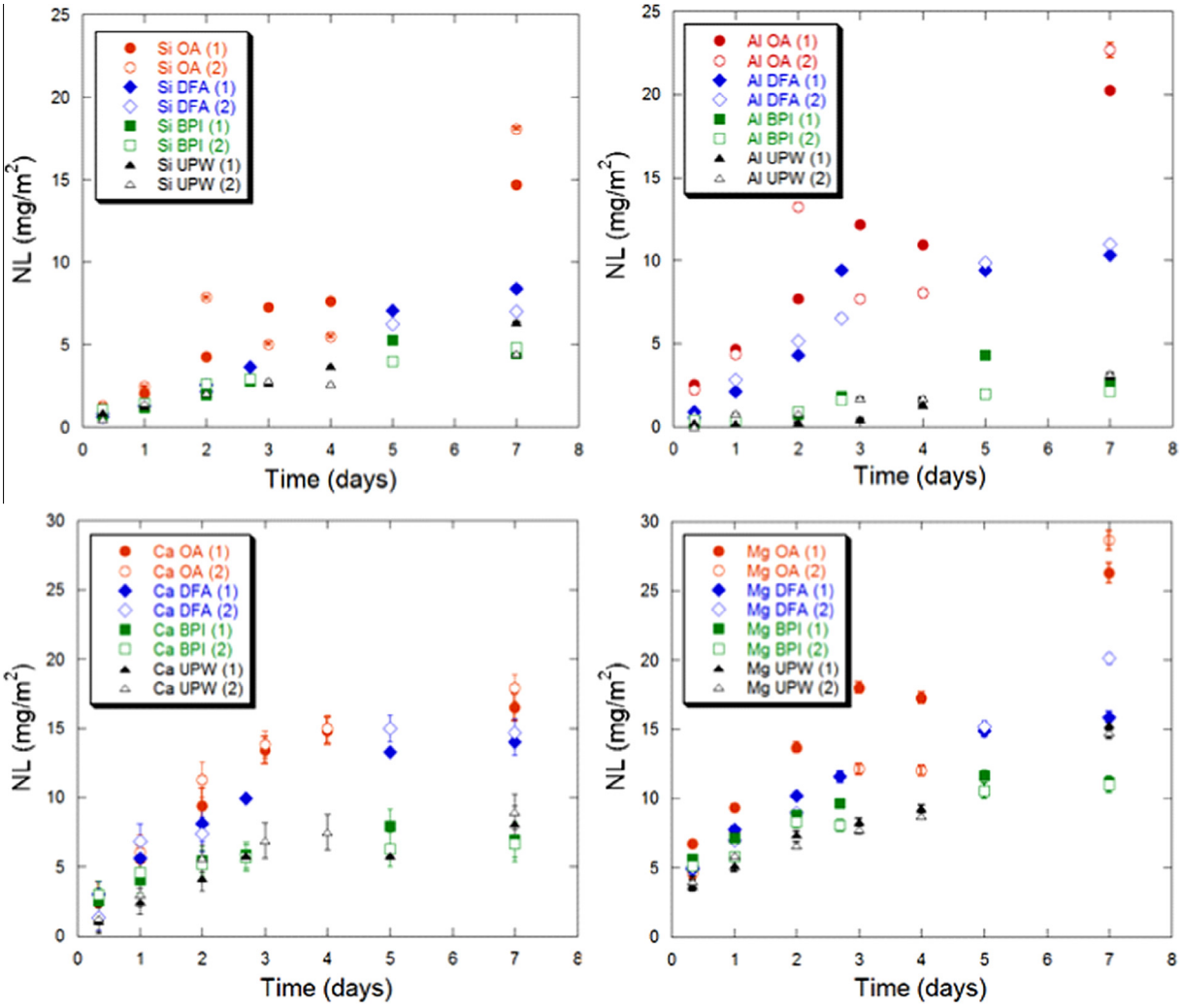

Fig. 2. Normalized mass-loss (NL) profiles of Si, Al, Ca and Mg during experiments performed on HAPLO glass at 25 °C and pH 6.4 in the presence of oxalic acid (OA), desferrioxamine (DFA), 2,2′-bibyridyl ′(BPI) or in ultrapure water (UPW) only. Full and empty symbols represent the first (1) and second (2) sets of experiments, respectively. For each NL value, the absolute error is calculated from the technical relative error in concentration.

Table 4
Si, Al, Fe, Ca and Mg initial dissolution rates calculated for each experimental conditions using the average of the first 4 NL values for sets (1) and (2) of experiments. Error bars bar are equal to ±2SD.

		Dissolution rates (mg m^{-2} d^{-1})				
		Si	Al	Fe	Ca	Mg
MORB	UPW	0.5 ± 0.1	0.5 ± 0.1	0	1.0 ± 0.6	0.9 ± 0.0
	BPI	1.5 ± 0.1	0.6 ± 0.1	0.9 ± 0.1	5.5 ± 0.2	3.7 ± 0.1
	OA	2.0 ± 0.0	3.6 ± 0.1	3.6 ± 0.0	5.0 ± 0.0	2.3 ± 0.4
	DFA	2.1 ± 0.1	3.4 ± 0.2	3.8 ± 0.1	4.9 ± 0.4	4.1 ± 0.1
HAPLO	UPW	0.8 ± 0.0	0.4 ± 0.1	–	1.0 ± 0.4	1.5 ± 0.1
	BPI	0.9 ± 0.0	0.6 ± 0.0	–	1.4 ± 0.2	1.7 ± 0.1
	OA	2.0 ± 0.1	3.6 ± 0.3	–	3.6 ± 0.3	4.2 ± 0.2
	DFA	1.3 ± 0.0	2.5 ± 0.2	–	2.9 ± 0.0	2.7 ± 0.2

characterized by a fast initial release of Ca and Mg (in most cases >4.0 mg m^{-2} d^{-1}) but also of Fe and Al (around 3.5 mg m^{-2} d^{-1}) in solution. In these media, Si is characterized by the slowest initial dissolution rates

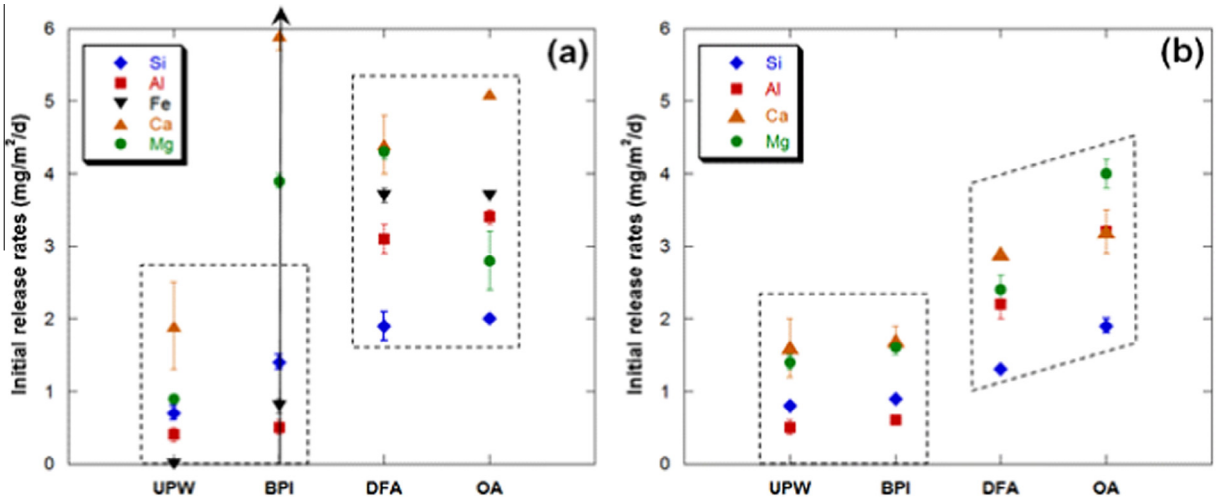

Fig. 3. Initial dissolution rates of MORB (a) and HAPLO (b) glasses in ultrapure water (UPW), 2,2′-bipyridyl (BPI), desferrioxamine (DFA) and oxalic acid (OA) solutions, calculated using the average of NL values for sets (1) and (2) of experiments. Error bars bar are equal to ±2SD.

(2.0 mg m^{-2} d^{-1}). Considering the experimental error on Mg release rate in OA solution, this element appears to be released more rapidly in the presence of DFA. Initial dissolution rates of MORB glass in BPI solutions are more comparable to those calculated in solutions without ligands. Al and Fe initial releases are slow and are very similar for the experiments with UPW and BPI solutions. However, Ca and Mg are released quickly (up to 5.5 mg m^{-2} d^{-1}) from the silicate network in the presence of BPI, while rates approach 1.0 mg m^{-2} d^{-1} in solutions without ligands.

Initial dissolution rates of HAPLO glass in the presence of BPI are all equivalent to those calculated for UPW solutions. In these experiments Ca and Mg are released the most rapidly, even though their dissolution rates do not exceed 1.7 mg m^{-2} d^{-1}. Si and Al are characterized by slow dissolution rates which do not reach 1.0 mg m^{-2} d^{-1}. In contrast, the calculated dissolution rates of HAPLO glasses in the presence of OA and DFA are slightly different, as the rates calculated for the experiments with the DFA solutions are systematically lower than those obtained for the OA experiments. For both DFA and OA, Mg, Ca and Al are released the most rapidly (around 3.5 mg m^{-2} d^{-1} for OA and 2.5 mg m^{-2} $d^{-1}$for DFA) whereas Si is released the most slowly.

One significant difference between MORB and HAPLO glass dissolution is the release of Mg in the presence of OA. Mg release rates are enhanced when the glass does not contain any iron.

3.3. Stoichiometry

The dissolution is non stoichiometric for both glasses regardless of the presence or absence of organic ligands (Table 5, Fig. 4).

Very similar values of $RRR_{X/Si}$ are calculated for the MORB glass in the presence of OA and DFA. Dissolution in those conditions is non stoichiometric for all elements with respect to Si, as it is characterized by a preferential release of Ca (>2) and also of Mg, Fe and Al (>1.5). In contrast, dissolution in the UPW and BPI solutions is characterized by a preferential release of Si with respect to Al and Fe. However, Ca and Mg are both preferentially released with respect to Si. A significant preferential release of Ca and Mg is recorded in the presence of BPI (>3.5).

HAPLO glass dissolution experiments in UPW and BPI solutions are characterized by similar $RRR_{X/Si}$. Si is preferentially released with respect to Al while Ca and Mg are preferentially released with respect to Si. In the presence

Table 5
Relative Release Ratios of Al, Fe, Ca and Mg by respect with Si calculated for each experimental conditions, using the average of NL values for sets (1) and (2) of experiments. Standard deviations are equal to ±2SD.

		$RRR_{Al/Si}$	$RRR_{Fe/Si}$	$RRR_{Ca/Si}$	$RRR_{Mg/Si}$
MORB	UPW	1.0 ± 0.3	Tends to 0	1.9 ± 0.1	1.8 ± 0.2
	BPI	0.5 ± 0.1	0.9 ± 0.1	5.4 ± 0.3	3.6 ± 0.3
	OA	1.8 ± 0.1	1.8 ± 0.0	2.5 ± 0.0	1.2 ± 0.2
	DFA	1.6 ± 0.0	1.8 ± 0.1	2.3 ± 0.0	1.9 ± 0.2
HAPLO	UPW	0.5 ± 0.1	–	1.2 ± 0.5	1.8 ± 0.1
	BPI	0.7 ± 0.0	–	1.7 ± 0.3	2.0 ± 0.1
	OA	1.8 ± 0.1	–	1.8 ± 0.1	2.2 ± 0.0
	DFA	2.0 ± 0.2	–	2.2 ± 0.0	2.2 ± 0.1

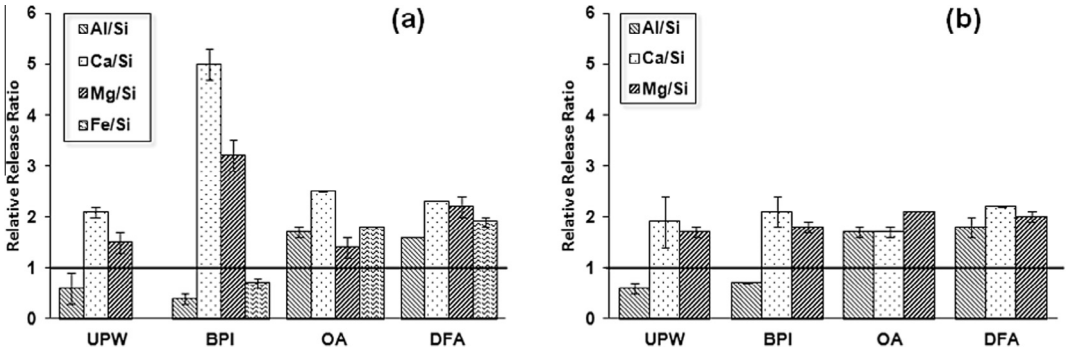

Fig. 4. Non-stoichiometric ratios calculated for MORB (a) and HAPLO (b) glasses in UPW, BPI, DFA and OA solutions using the average of NL values for sets (1) and (2) of experiments. Error bars bar are equal to ±2SD. The line materializes a stoichiometric release between Si and the considered elements.

of BPI, the high values of $RRR_{Ca/Si}$ and $RRR_{Mg/Si}$ obtained for the MORB glass are not observed for the HAPLO composition and approach non-stoichiometric ratios values calculated in UPW. Very similar values of $RRR_{X/Si}$ are calculated for the HAPLO glass in the presence of OA and DFA as Al, Ca and Mg are all preferentially released with respect to Si, and their respective ratios all approach 2.

In summary, calculated initial dissolution rates of MORB and HAPLO glasses in UPW (Table 4) show high Mg and Ca and low Al and Si release. This is in good agreement with the mechanism proposed by Oelkers (2001) in which the first step of basaltic glass dissolution in acidic water is the fast and almost complete removal of divalent cations such as Ca or Mg. Dissolution rates in the presence of organic molecules differ from those in the presence of UPW demonstrating the impact of the ligands on the alteration process.

4. DISCUSSION

4.1. Effect of solution on the basaltic glass dissolution

4.1.1. Effect of ligands

One major difference between dissolution profiles in non-ligand and ligand-bearing solutions is the preferential release of trivalent cations of the glass with respect to Si in the presence of OA and DFA, and an enhanced relative release of divalent species in the presence of BPI (Fig. 4a). This effect is particularly significant for Fe dissolution profiles in the presence of OA or DFA. In experiments without ligands, iron was not detectable (the detection limit of Fe was evaluated as 2 ppb). However, in presence of trivalent cation-complexing ligands (OA and DFA), Fe was present in sufficient amounts to be detected and was systematically released preferentially to Si. A similar behavior of iron was observed in hornblende dissolution experiments in the presence or absence of DFA (Kalinowski et al., 2000a).

This can be explained by the fact that OA-Fe^{3+} and DFA-Fe^{3+} form stable aqueous complexes. More generally, organic ligands that have the strongest equilibrium constants are more effective in enhancing corresponding dissolution rates (Fig. 3a). This is in good agreement with previous dissolution studies with multioxides (Schott et al., in Oelkers and Schott, 2009) or bunsenite (Ludwig et al., 1995), granite and basaltic glass (Hausrath et al., 2009). This correlation is notably verified considering the release of elements from the glass in the presence of either DFA and OA or BPI. DFA and OA, which can form the most stable and the strongest complexes with Fe^{3+} and Al^{3+}, are extremely efficient in promoting MORB dissolution. In contrast, the experiments with BPI, which does not have affinity for Fe^{3+} or Al^{3+}, and in general with trivalent cations, exhibit cation releases similar to those with UPW.

Despite contrasting complexation constants, the DFA, OA and BPI experiments exhibit similar Ca and Mg release rates (Table 4, MORB). In contrast, the RRRs calculated for the BPI experiments are different from those for the OA and DFA experiments (Table 5). In the presence of DFA and OA, the enhancement of Ca and Mg release correlates with the release of Si, suggesting that both Ca and Mg release results from the dissolution of the silicate network. By contrast, while BPI has a slightly smaller impact on Si release by comparison with DFA and OA, Ca and Mg release in this solution is greatly increased (Table 5). For the BPI experiments, Ca and Mg extraction from the glass network may be driven by an interaction between these elements and the BPI molecules. This interpretation is not supported by values of the complex formation constants (Table 6) but it is supported by the highest pH values

Table 6
(1:1) Complex formation constants of oxalate, desferrioxamine and 2,2′-bipyridyl with major elements from the glass.

	OA	DFA	BPI
Al^{3+}	$10^{7.1}$ [a]	$10^{24.1}$ [c]	–
Fe^{3+}	10^{8} [a]	$10^{30.6}$ [c]	–
Fe^{2+}	$10^{4.7}$ [a]	$10^{9.0}$ [c]	$10^{17.5}$ [d]
Ca^{2+}	$10^{3.0}$ [a]	$10^{2.6}$ [c]	$10^{-0.05}$ [d]
Mg^{2+}	$10^{3.4}$ [b]	$10^{2.8}$ [e]	$10^{0.32}$ [d]

[a] Cama and Ganor, 2006.
[b] Grases et al., 1989.
[c] Kraemer, 2004.
[d] Capone et al., 1985.
[e] Farkas et al., 1999.

in the BPI experiments, which suggests that a chemisorption reaction occurred between the glass and BPI, as has been observed on clay and oxides (Ferreiro et al., 1983; Ferreiro and Bussetti, 2007).

4.1.2. Ligand concentrations and saturation effect

OA and DFA both increase the dissolution rate of most of the studied elements from the glass (Fig. 3a). These impacts agree with those determined in mineral weathering studies performed in the presence of OA and DFA ligands (Welch and Ullman, 1992; Watteau and Berthelin, 1994; Stillings et al., 1995; Liermann et al., 2000; Cheah et al., 2003; Rosenberg and Maurice, 2003; Wolff-Boenish et al., 2011; Rozalen et al., 2013). However, the fact that DFA is ten times more diluted than OA, and the assumption that the dissolution rates at fixed pH depend linearly on the concentrations of adsorbed ligands and therefore on the concentrations of ligands in the solution, suggest that DFA is more powerful than OA in promoting basaltic glass dissolution. Similar conclusions were drawn in a study about hematite dissolution in the presence of OA and a Fe(III) – specific siderophore (Hersman et al., 1995).

One DFA molecule is sufficient to complex trivalent cations such as Fe^{3+} and Al^{3+}, while three OA molecules are required to form a highly stable complex (Wolff Boenisch and Traina, 2007). Experimental studies have demonstrated that $Fe(oxalate)^{2-}$ is the predominant Fe-oxalate species (Cervini-Silva, 2012), whereas DFA coordinates to an individual Fe site via one or two of its chelating groups (Holmen and Casey, 1996; Cocozza, 2002) instead of completing the octahedral coordination sphere of the Fe(III) in a 1:1 complex. As a consequence, and assuming equivalent efficiencies, OA should be at least 3 times more concentrated than DFA to promote the release of Fe^{3+} and Al^{3+} in the same manner as DFA. This is not in accordance with our experimental results, which show similar dissolution rates for Al and Fe (Table 4) despite the OA and DFA concentrations differing by one order of magnitude. A similar discrepancy between the expected and observed results was observed in a study on goethite dissolution in the presence of either DFA or acetohydroxamic acid (Holmen and Casey, 1996). These discrepancies might be related to a possible saturation effect at the glass-fluid interface. At high ligand concentrations, ligands which are not in the first adsorption layer, *i.e.* which do not interact directly with surface cations, might not affect the release of those elements from the glass (Furrer and Stumm, 1986), and might even decrease the possible effect of ligands on cation solubilities, stopping the cations from being removed (Kraemer, 2004). Previous studies have shown that goethite dissolution rates reach a plateau at OA concentrations above 5 mM (Cheah et al., 2003) and 1 mM (Wolff-Boenisch and Traina, 2006). Considering the respective specific surface area and bulk concentration of their material, the number of OA molecules ideally adsorbed per surface unit of goethite (without taking into account possible steric constraints) would range from 2.9 to 14.3 μmol m^{-2}. This saturation effect might also exist when dissolution experiments are performed in the presence of highly specific siderophores (Kalinowski et al., 2000b). In their work on DFA adsorption on goethite, Kraemer et al. (1999) measured the maximum surface concentrations of DFA as >0.4 μmol m^{-2}. In our study, with a specific surface of 0.04 m^2 g^{-1}, the number of OA molecules ideally adsorbed per surface units of glass is 1200 μmol m^{-2}, whereas the number of DFA molecules ideally adsorbed per surface units of glass is 120 μmol m^{-2}. These preliminary calculations suggest that the surface of both glasses is largely oversaturated with ligands compared to those in these other studies. This could explain the similar dissolution rates calculated for OA and DFA solutions, despite the fact that DFA is 10 times more diluted than OA. Ligands molecules remaining in solution might be involved in the chelation of dissolved metal cations, causing an increase in the apparent solubility of the solid and thus enhancing its dissolution. This ligand-promoted dissolution mechanism occurring in solution has been presented by Oelkers and Schott (1998) as an alternative to the generally accepted surface-controlled dissolution mechanism (Stillings et al., 1998; Rosenberg and Maurice, 2003; Cama and Ganor, 2006).

In natural systems, organic molecules typically exhibit a lower range of concentrations compared to those studied here, meaning that the magnitude of this ligand-promoted dissolution may be in reality restricted. The low abundance of dissolved oxalate in the environment can be due to the low solubility (and thus precipitation) of calcium oxalate. Oxalate is generally present in soils at concentrations up to 1 mM L^{-1} (Fox and Comerford, 1990). In marine systems, reported concentrations of siderophores vary between 0.3 and 7 nM (Kraemer, 2004). However, it has been speculated that close to the interface between micro-organisms and solid phases, the local concentrations of organic ligands and of siderophores can locally increase by several orders of magnitudes (Ahmed and Holmström, 2014). For a bacterial microniche, siderophore concentrations are indeed expected from 10 μM to few mM (Hersman et al., 1995).

4.2. Effect of glass structure

4.2.1. Silica glass former and modifier cations

Si is a major network-forming element in the glass structure and the rupture of Si–O–X (X = Si, Al, Fe) bonds in the network is considered as the rate-limiting step in dissolution (Oelkers, 2001). The possible role played by organic ligands and particularly by OA on silica release is not well understood, even in crystalline materials. Studies on quartz dissolution conclude that while Si dissolution rates are enhanced by the presence of OA (Benett et al.,1988), the complexation of Si by OA is not the driving force for the quartz dissolution (Bennett, 1991). This conclusion is further corroborated by the fact that quartz solubility is almost identical in different carboxylic acid solutions (Franklin et al., 1994). Consequently, the effect of Si complexation by OA on the dissolution of our glass samples was assumed to be negligible, and the increase in Si dissolution rates in the presence of OA, DFA and BPI was attributed to the destabilization of the Si network by the complexation and transfer to solution of metallic cations at the glass surface.

In the presence of either OA or DFA, the increase in Si dissolution rates (Fig. 3) correlates well to the preferential extraction of Fe^{3+} and Al^{3+} in OA/DFA solutions as compared to the rates in the UPW experiments (Fig. 4). By contrast the $RRR_{Ca/Si}$ and $RRR_{Mg/Si}$ remain constant in all these cases, indicating that these ligands do not affect the dissolution mechanism. The interaction between Fe^{3+} and Al^{3+} and OA or DFA, combined with the network-forming role of these trivalent cations in the glass structure, might be responsible for weakening and consequently enhancing the dissolution of the whole silicate network.

In the presence of BPI, Mg and Ca are preferentially extracted from the glass with respect to Si. Concomitantly, $RRR_{Fe/Si}$ is much stronger in BPI (0.9) than in UPW (0). A possible complexation of Fe(III) by BPI was described in Nord and Wernberg (1975), who concluded that in the presence of BPI, Fe(III) was rapidly reduced by hydroxide ions according to the following the reaction:

$$4Fe(BPI)_3^{3+} + 4OH^- = 4Fe(BPI)_3^{2+} + O_2 + 2H_2O$$

Templeton (2002) attributed a high complex formation constant between BPI and Fe(III) ($10^{16.3}$). Our OA and DFA results suggest that such a high constant should have resulted in higher Fe relase rates. This raises the question of a possible interaction between the BPI molecules and Fe(II) from the glass. As previously mentioned, although Fe(III) is the predominant valence in the prepared MORB glass, Fe(II) could indeed represent up to 30% of the total concentration of iron in the solid. The very strong affinity between BPI and Fe^{2+} cations (Table 6) could thus also explain the promoted dissolution of the MORB glass in BPI solution as compared to UPW. However, due to their modifier role in the glass structure, the impact of neither Ca and Mg or Fe preferential release on Si dissolution rate is expected to be very strong.

As Fe, under its reduced or oxidized form, obviously has a key-role in ligand-promoted mechanisms, the comparison with the HAPLO glass – i.e., a glass without any form of iron - dissolution process appears to be necessary to have access to complementary information and to precisely identify the reactions involved.

4.2.2. Composition of the glass

4.2.2.1. Oxalic acid and ligand-free solutions. In the OA and UPW experiments, the presence or absence of iron in the glass does not seem to have any effect on dissolution rates and stoichiometry (Fig. 5).

Similar dissolution profiles for the MORB and HAPLO glasses were observed. It is expected that UPW does not induce any detectable Fe dissolution from the MORB glass (Fig. 3) and that, despite small differences in their composition, the MORB and HAPLO glasses are involved in the same dissolution reactions. In the case of OA, the very similar trend in the Al and Si dissolution profiles in the presence or absence of Fe in the glass suggests that Fe^{3+} removal has no impact on basaltic glass dissolution. Consequently, complexation and release of Al from both glasses could be the rate-limiting steps of the OA promoted dissolution, despite OA being able to complex Fe^{3+} as easily as Al^{3+} (Table 6) and both Al and Fe(III) being involved as formers in the glass structure. This interpretation is in agreement with several studies on Fe(II)-bearing basaltic glass dissolution (Oelkers et al., 1994; Oelkers, 2001; Oelkers and Gislason, 2001). Whatever the oxidation state of Fe (mostly oxidized in this work) and its role in the glass structure, it seems that the first step in the dissolution of alumino-silicates is the fast exchange of alkaline and alkaline earth elements of the glass with the protons of the solution. This fast removal is followed by slower hydrolysis of Al–O–Si bonds, which are relatively weak compared to Si–O–Si bonds. This is considered as the rate-limiting step of the dissolution process, weakening the silicate network and facilitating the final hydrolysis of Si–O–Si bonds. This mechanism was shown by Oelkers and Gislason (2001) to occur with or without oxalic acid in solution. The presence of oxalic acid only increases the removal of Al, thus accelerating the dissolution process.

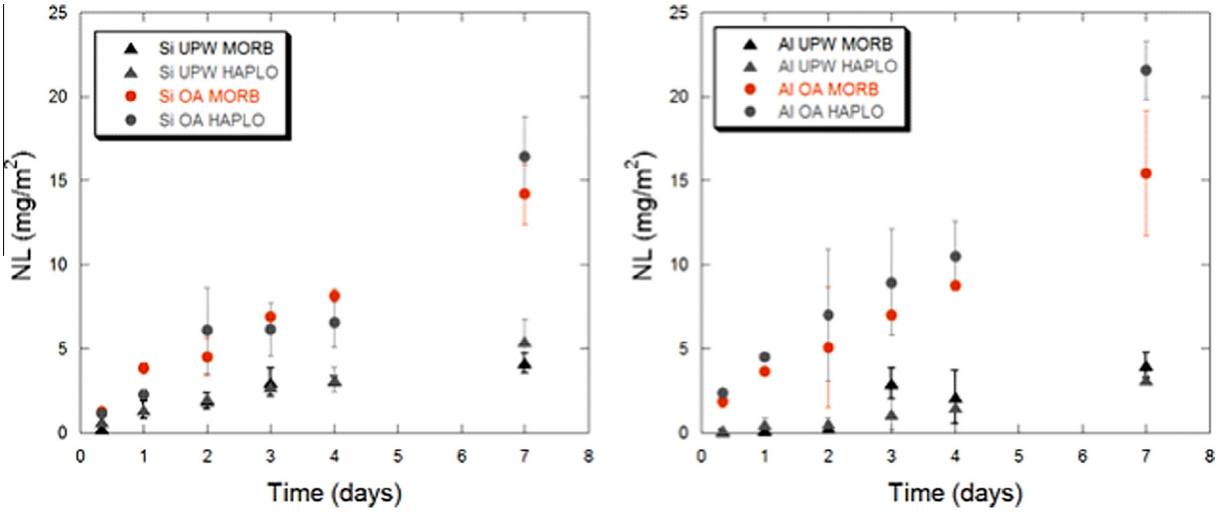

Fig. 5. Normalized Loss profiles of Si and Al during experiments performed on MORB and HAPLO glasses in the presence of oxalic acid (OA) or in ultrapure water (UPW) only, using the average of NL values for sets (1) and (2) of experiments. Error bars bar are equal to ±2SD.

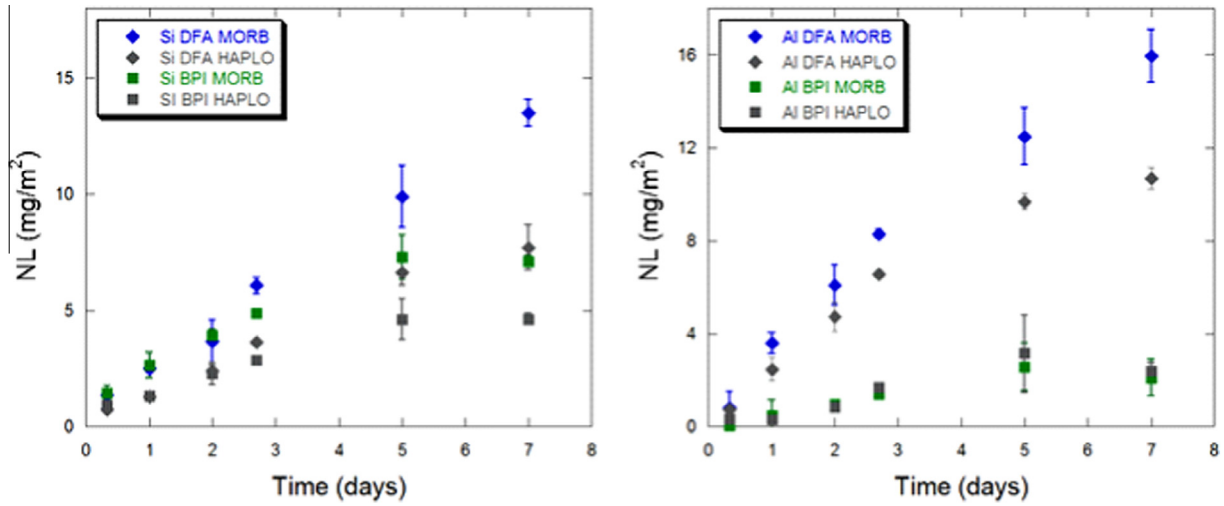

Fig. 6. Normalized Loss profiles of Si and Al during experiments performed on MORB and HAPLO glasses in the presence of desferrioxamine (DFA) or 2,2′-bipyridyl (BPI), using the average of NL values for sets (1) and (2) of experiments. Error bars bar are equal to ±2SD.

One difference between the MORB and HAPLO dissolution profiles in the presence of OA is the high amounts of Mg released (Fig. 3). Considering that the major difference between the respective compositions of MORB and HAPLO glasses was the percentage of Mg – 7.7 wt.% in MORB versus 15.2 wt.% in HAPLO (Table 1) – this increase in dissolution rates shows the impact of glass composition on the dissolution reaction.

4.2.2.2. Desferrioxamine. In DFA solutions, the absence of Fe in the glass correlates with a decrease in all dissolution rates (Fig. 6).

This indicates that DFA-Fe^{3+} complex formation plays a significant role in the ligand-promoted dissolution process, in contrast with the OA and UPW experiments. The very high constant characterizing the complexation of Fe(III) by DFA (6 orders of magnitude higher than DFA-Al^{3+} formation constant) (Table 6) suggests that Fe(III) might be involved in promoting Si–O–Si detachment and in catalyzing the dissolution process. Despite the decrease in rates in the absence of Fe, the RRRs remain similar between MORB and HAPLO glasses (Fig. 4). This indicates that, even if their release from the glass is slower, elements are still following the same dissolution pattern, typical of a ligand promoted mechanism. Despite high DFA-Al^{3+} complex formation constants, Al complexation and release is probably the main mechanism promoting the dissolution process of the HAPLO glass, as observed in OA experiments performed on both MORB and HAPLO and in the work of Oelkers and Gislason (2001).

4.2.2.3. 2,2′-Bipyridyl. The releases of all elements from the Fe-free glass in the presence of BPI appear to be slower than those from the MORB glass (Fig. 6). Moreover, dissolution experiments carried out on the HAPLO glass are characterized by rates and stoichiometry which are very similar to those calculated in the ligand-free experiments (Figs. 3a and 4a). This general decrease, together with the similarity of the dissolution profiles for the UPW or BPI experiments for the HAPLO glass, implies that in the absence of iron in the glass, the presence of BPI has no impact on the dissolution process. This confirms the significant role of BPI-Fe^{2+} complexes and suggests the absence of significant BPI-Al^{3+} interactions. Even though Fe(II) is not the dominant valence of iron in the MORB glass, its release thus plays a significant role in promoting the global dissolution of the glass.

5. CONCLUSION AND PERSPECTIVES

The dissolution kinetics of basaltic glass were investigated with respect to the role and impact of iron in glass and the type of dissolution solution by performing experiments with Fe(II) and/or Fe(III) specific chelators having various complex formation constants, and by using two compositions of glasses. The effects observed are in agreement with ligand-promoted dissolution mechanisms described for several minerals in the literature. In the presence of OA and DFA, the preferential release of trivalent cations promoted the whole glass dissolution. In the case of OA, however, Al release is thought to promote the dissolution of both glasses, whereas in the case of DFA the preferential release of Fe(III) is responsible for the enhanced dissolution of MORB glass. In BPI solution, the MORB dissolution seems to be driven by the Fe(II) release despite its low content in the glass.

To go further in the determination of elementary mechanisms and of their implications in natural systems, complementary issues need to be addressed. The impact of ligands on MORB dissolution has to be studied using variable concentrations. This will allow to investigate both the effect of concentrations closer to the ones found in the natural field but also the possible existence of threshold values that will provide information about the localization of the ligand promoted dissolution (surface or bulk solution). Being a preliminary step to future work with microorganisms, the present study was dedicated to Fe(III)-bearing glass in order to highlight the central role of Fe, under its oxidized

form, in ligand-promoted dissolution mechanisms. The role of Fe(II) in the ligand promoted dissolution and particularly in the presence of BPI will be further investigated on Fe(II)-bearing glasses that are more representative of natural basalts, in order to have a global overview of basaltic glass dissolution and precise the mechanisms occurring in nature. Finally, the characterization of the alteration layers (calculated as being of 35–150 Å in thickness) and of minute amount of secondary phases will be an important step to be addressed in a separate study. The effect of complexing agents in longer-term experiments, and notably their effect on the passivating properties of the gel layer, should also be investigated. The precise knowledge of the abiotic reactions occurring in the simplified systems considered in this work is indeed an essential step before addressing the study of alteration processes in presence of microorganisms, major actors of natural systems.

ACKNOWLEDGEMENTS

The authors are very grateful to the reviewers for their constructive comments and to Karen Hudson-Edwards (DEPS, Birkbeck School/UCL) for her precious help in editing the revised manuscript. The authors would like to thank Jessica Ferrand (LGE) for her help during glass preparation and Lola Sarrasin (master student) for helping setting up the dissolution experiments. Rossana Combes (LGE) is warmly acknowledged for taking part in all ICP analysis sessions and collaborating in the uncertainty determination work. Stéphanie Blanchandin's help in ATD measurement at Soleil Synchrotron was also much appreciated. The authors would also like to thank Céline Rommevaux-Jestin (IPGP) and Jérôme Labanowski (CNRS, Université de Poitiers) for fruitful discussions. This work was supported by grants from Region Ile de France and by CNRS-INSU.

REFERENCES

Abdelouas A., Crovisier J. L. and Lutze W. (1993) Hydrotalcite formation by alteration of R7T7 nuclear waste glass in a salt solution at 190 °C. *C. r. Acad. sci.* **317**, 1067–1072.

Ahmed E. and Holmström S. J. M. (2014) The effect of soil horizon and mineral type on the distribution of siderophores in soil. *Geochim. Cosmochim. Acta* **131**, 184–195.

Aouad G., Crovisier J. L., Geoffroy V. A., Meyer J. M. and Stille P. (2006) Microbially-mediated glass dissolution and sorption of metals by *Pseudomonas aeruginosa* cells and biofilm. *J. Hazard. Mater.* **B136**, 889–895.

Bennett P. C. (1991) Quartz dissolution in organic-rich aqueous systems. *Geochim. Cosmochim. Acta* **55**, 1781–1797.

Bennett P. C., Melcer M. E., Siegel D. I. and Hassett J. P. (1988) The dissolution of quartz in dilute aqueous solutions of organic acids at 25 °C. *Geochim. Cosmochim. Acta* **52**, 1521–1530.

Brandel J., Humbert N., Elhabiri M., Schalk I. J., Mislin G. L. A. and Albrecht-Gary A. M. (2012) Pyochelin, a siderophore of *Pseudomonas aeruginosa*: physicochemical characterization of the iron(III), copper(II) and zinc(II) complexes. *Dalton Trans.* **41**, 2820–2834.

Braud A., Hoegy F., Jézéquel K., Lebeau T. and Schalk I. J. (2009) New insights into the metal specificity of the *Pseudomonas aeruginosa* pyoverdine-iron uptake pathway. *Environ. Microbiol.* **11**, 1079–1091.

Brunauer S., Emmett P. H. and Teller E. (1938) Adsorption of gases in multimolecular layers. *J. Am. Chem. Soc.* **60**, 309–319.

Cagno S., Nuyts G., Bugani S., de Vis K., Schalm O., Caen J., Helfen L., Cotte M., Reischiq P. and Janssens K. (2011) Evaluation of manganese-bodies removal in historical stained glass windows vi SR-μ-XANES/XRF and SR-μ-CT. *J. Anal. At. Spectrom.* **26**, 2442–2451.

Cama J. and Ganor J. (2006) The effects of organic acids on the dissolution of silicate minerals: a case study of oxalate catalysis of kaolinite dissolution. *Geochim. Cosmochim. Acta* **70**, 2191–2209.

Capone S., De Robertis A., De Stefano C. and Scarcella R. (1985) Thermodynamics of formation of magnesium, calcium, strontium and barium complexes with 2,2′-bipyridyl and 1,10-phenanthroline, at different ionic strengths in aqueous solution. *Talanta* **32**, 675–677.

Cervini-Silva J., Kearns J. and Banfield J. (2012) Steady-state dissolution kinetics of mineral ferric phosphate in the presence of desferrioxamine-B and oxalate ligands at pH = 4–6 and T = 24 ± 0.6 °C. *Chem. Geol.* **320–321**, 1–8.

Cheah S. F., Kraemer S. M., Cervini-Silva J. and Sposito G. (2003) Steady-state dissolution kinetics of goethite in the presence of desferrioxamine-B and oxalate ligands: implications for the microbial acquisition of iron. *Chem. Geol.* **198**, 63–75.

Chou L. and Wollast R. (1984) Study of weathering of albite at room temperature and pressure with a fluidized bed rector. *Geochim. Cosmochim. Acta* **48**, 2205–2217.

Cocozza C., Tsao C. C. G., Cheah S. F., Kraemer S. M., Raymond K. N., Miano T. M. and Sposito G. (2002) Temperature dependence of goethite dissolution promoted by trihydroxamate siderophores. *Geochim. Cosmochim. Acta* **66**, 431–438.

Coluccia S., Chiorino A., Guglielminotti E. and Morterra C. (1978) Adsorption of 2,2′-bipyridyl on magnesium oxide and calcium oxide. *J. Chem. Soc., Faraday Trans.* **1**(75), 2188–2198.

Crovisier J. L., Advocat T. and Dussossoy J. L. (2003) Nature and role of natural alteration gels formed on the surface of ancient volcanic glasses (Natural analogs of waste containment glasses). *J. Nucl. Mater.* **321**, 91–109.

Curti E., Crovisier J. L., Morvan G. and Karpoff A. M. (2006) Long-term corrosion of two nuclear waste reference glasses (MW and SON68): a kinetic and mineral alteration study. *Appl. Geochem.* **21**, 1152–1168.

Daux V., Guy C., Advocat T., Crovisier J. L. and Stille P. (1997) Kinetic aspects of basaltic glass dissolution at 90 °C: role of aqueous silicon and aluminium. *Chem. Geol.* **142**, 109–126.

Drever J. I. and Stillings L. L. (1997) The role of organic acids in mineral weathering. *Colloids Surf.* **120**, 167–181.

Drewello R. and Weissmann R. (1997) Microbially influenced corrosion of glass. *Appl. Microbiol. Biotechnol.* **47**, 337–346.

Elandalloussi L. (2003) Effect of desferrioxamine and 2,2′-bipyridyl on the proliferation of *Perkinsus atlanticus*. *Biomol. Eng.* **20**, 349–354.

Farkas E., Enyedy E. A. and Csoka H. (1999) A comparison between the chelating properties of some dihydroxamic acids, desferrioxamine B and acetohydroxamic acid. *Polyhedron* **18**, 2391–2398.

Ferreiro E. A., Bussetti S. G. and Helmy A. K. (1983) Sorption of 2,2′-bipyridine on clays and oxides. *Z. Planzenernaehr. Bodenk.* **146**, 369–378.

Ferreiro E. A. and Bussetti S. G. (2007) Thermodynamic parameters of adsorption of 1,10-phenanthroline and 2,2′-bipyridyl on hematite, kaolinite and montmorillonites. *Colloids Surf.* **301**, 117–128.

Fliegel D., Knowles E., Wirth R., Templeton A., Staudigel H., Muehlenbachs K. and Furnes H. (2012) Characterization of alteration textures in Cretaceous oceanic crust (pillow lava) from the N-Atlantic (DSDP Hole 418A) by spatially-resolved spectroscopy. *Geochim. Cosmochim. Acta* **96**, 80–93.

Fournier M., Gin S. and Frugier P. (2014) Resumption of nuclear glass alteration: state of the art. *J. Nucl. Mater.* **448**, 348–363.

Fox T. R. and Comerford N. B. (1990) Low molecular-weight organic acids in selected forest soils of the southeastern USA. *Soil Sci. Soc.* **54**, 1139–1144.

Franklin S. P., Hajash A. J., Dewers T. A. and Tieh T. T. (1994) The role of carboxylic acids in albite and quartz dissolution: an experimental study under diagnetic conditions. *Geochim. Cosmochim. Acta* **57**, 4259–4279.

Furrer G. and Stumm W. (1986) The coordination chemistry of weathering: I. Dissolution kinetics of δ-Al_2O_3 and BeO. *Geochim. Cosmochim. Acta* **50**, 1847–1860.

Gallien J. P., Gouget B., Carrot F., Orial F. and Brunet A. (2001) Alteration of glasses by micro-organisms. *Nucl. Instrum. Methods Phys. Res. B* **181**, 610–615.

Galeczka I., Wolff-Boenisch D., Oelkers E. H. and Gislason S. R. (2014) An experimental study of basaltic glass-H_2O-CO_2 interaction at 22 and 50 °C: implications for subsurface storage of CO_2. *Geochim. Cosmochim. Acta* **126**, 123–145.

Gentaz L. (2011) *Simulation et modélisation de l'altération des verres de composition médiévale dans l'atmosphère urbaine* Thèse de doctorat. Université Paris-Est, 264 p.

GERM (2000) The Geochemical Earth Reference Model, http://EarthRef.org/agenda.htm.

Gin S., Beaudoux X., Angéli F., Jégou C. and Godon N. (2012) Effect of composition on the short-term and long-term dissolution rates of ten borosilicate glasses of increasing complexity from 3 to 30 oxides. *J. Non-cryst. Solids* **358**, 2559–2570.

Gin S., Frugier P., Jollivet P., Bruguier F. and Curti E. (2013) New insight into the residual rate of borosilicate glasses: effect of S/V and glass composition. *Int. J. Appl. Glass Sci.* **4**, 371–382.

Gin S., Abdelouas A., Criscenti L. J., Ebert W. L., Ferrand K., Geisler T., Harrison M. T., Inagaki Y., Mitsui S., Mueller K. T., Marra J. C., Pantano C. G., Pierce E. M., Ryan J. V., Schofiel J. M., Steefel C. I. and Vienna J. D. (2014) An international initiative on long-term behavior of high-level nuclear waste glass. *Mater. Today* **16**, 243–248.

Gin S., Jollivet P., Fournier M., Angeli F., Frugier P. and Chapentier T. (2015) Origin and consequences of silicate glass passivation by surface layers. *Nat. Commun.* **6**, 6360.

Gislason S. R. and Oelkers E. H. (2003) Mechanism, rates and consequences of basaltic glass dissolution: II. An experimental study of the dissolution rates of basaltic glass as a function of pH and temperature. *Geochim. Cosmochim. Acta* **67**, 3817–3832.

Gislason S. R., Oelkers E. H., Eiriksdottir E. S., Kardjilov M. I., Gisladottir G., Sigfusson B., Snorrason A., Elefsen S., Hardardottir J., Torssander P. and Oskarsson N. (2009) Direct evidence of the feedback between climate and weathering. *Earth Planet. Sci. Lett.* **277**, 213–222.

Godon N., Thomassin J. H. and Touray J. C. (1988) Experimental alteration of R7T7 nuclear-model glass in solutions with different salinities (90 °C, 1 bar) – implications for the selection of geological repositories. *J. Mater. Sci.* **23**, 126–134.

Gorbushina A. A. and Palinska K. A. (1999) Biodeteriorative processes on glass: experimental proof of the role of fungi and cyanobacteria. *Aerobiologia* **15**, 183–191.

Grambow B. (1985) A general rate equation for nuclear waste glass corrosion. *Mater. Res. Soc. Symp. Proc.* **44**, 15–27.

Grases F., Genestar C. and Millan A. (1989) The influence of some metallic ions and their complexes on the kinetics of crystal growth of calcium oxalate. *J. Cryst. Growth* **94**, 507–512.

Hausrath E. M., Neaman A. and Brantley S. L. (2009) Elemental release rates from dissolving basalt and granite with and without organic ligands. *Am. J. Sci.* **309**, 633–660.

Hellmann R., Cotte S., Cadel E., Malladi S., Karlsson L. S., Lozano-Perez S., Cabié M. and Seyeux A. (2015) Nanometre-scale evidence for interfacial dissolution-reprecipitation control of silicate glass corrosion. *Nat. Mater.* **14**, 307–311.

Hernlem B. J., Vane L. M. and Sayles G. D. (1996) Stability constants for complexes of the siderophore desferrioxamine B with selected heavy metal cations. *Inorg. Chim. Acta* **244**, 179–184.

Hersman L., Lloyd T. and Sposito G. (1995) Siderophore-promoted dissolution of hematite. *Geochim. Cosmochim. Acta* **16**, 3327–3330.

Holdren G. R. and Speyer P. M. (1985) Reaction rate-surface area relationships during the early stages of weathering—I initial observations. *Geochim. Cosmochim. Acta* **49**, 675–681.

Holmen B. A. and Casey W. H. (1996) Hydroxamate ligands, surface chemistry, and the mechanism of ligand-promoted dissolution of goethite [≡ −FeOOH (s)]. *Geochim. Cosmochim. Acta* **60**, 4403–4416.

Hutchens E. (2009) Microbial selectivity on mineral surfaces: possible implications for weathering processes. *Fungal Biol. Rev.* **23**, 115–121.

Jollivet P., Angeli F., Cailleteau C., Devreux F., Frugier P. and Gin S. (2008) Investigation of gel porosity clogging during glass leaching. *J. Non-cryst. Solids* **354**, 4952–4958.

Kalinowski B. E., Liermann L. J., Brantley S. L., Barnes A. and Pantano C. G. (2000a) X-Ray photoelectron evidence for bacteria-enhanced dissolution of hornblende. *Geochim. Cosmochim. Acta* **64**, 1331–1343.

Kalinowski B. E., Liermann L. J., Givens S. and Brantley S. L. (2000b) Rates of bacteria-promoted solubilization of Fe from minerals: a review of problems and approaches. *Chem. Geol.* **169**, 357–370.

Knauss K. G., Johnson J. W. and Steefel C. I. (2005) Evaluation of the impact of CO_2, co-contaminant gas, aqueous fluid and reservoir rock interactions on the geologic sequestration of CO_2. *Chem. Geol.* **217**, 339–350.

Knowles E., Staudigel H. and Templeton A. (2013) Geochemical characterization of tubular alteration features in subseafloor basalt glass. *Earth Planet. Sci. Lett.* **374**, 239–250.

Kraemer S. M. (2004) Iron oxide dissolution and solubility in the presence of siderophores. *Aquat. Sci.* **66**, 3–18.

Kraemer S. M., Cheah S. F., Zapf R., Xu J., Raymond K. N. and Sposito G. (1999) Effect of hydroxamate siderophores on Pb(II) adsorption and Fe release by goethite. *Geochim. Cosmochim. Acta* **63**, 3003–3008.

Libourel G., Verney-Carron A., Morlok A., Gin S., Sterpenich J., Michelin A., Neff D. and Dillmann P. (2011) The use of natural and archeological analogues for understanding the long-term behavior of nuclear glasses. *C. R. Géosci.* **343**, 237–245.

Liermann L. J., Kalinowski B. E., Brantley S. L. and Ferry J. G. (2000) Role of bacterial siderophores in dissolution of hornblende. *Geochim. Cosmochim. Acta* **64**, 587–602.

Lombardo T., Gentaz L., Verney-Carron A., Chabas A., Loisiel C., Neff D. and Leroy E. (2013) Characterization of complex alteration layers in medieval glasses. *Corros. Sci.* **72**, 10–19.

Luckscheiter B. and Nesovic M. (2004) Short-term corrosion of HLM glass in aqueous solutions enriched with various metal cations. *J. Nucl. Mater.* **327**, 182–187.

Ludwig C., Casey W. H. and Rock P. A. (1995) Prediction of ligand-promoted dissolution rates from the reactivities of aqueous complexes. *Nature* **375**, 44–47.

Martinez-Luevanos A., Rodriguez-Delgado M. G., Uribe-Salas A., Carillo-Pedroza F. R. and Osuna-Alarcon J. G. (2011) Leaching kinetics of iron from low grade kaolin by oxalic acid solutions. *Appl. Clay Sci.* **51**, 473–477.

Michelin A., Burger E., Rebiscoul D., Neff D., Bruguier F., Drouet E., Dillmann P. and Gin S. (2013) Silicate glass alteration enhanced by iron: origin and long-term implications. *Environ. Sci. Technol.* **47**, 750–756.

Nord G. and Wernberg O. (1975) Reduction of tris(2,2′-bipyridyl) and tris(1,10-phananthroline) complexes of iron(III) and osmium(III) by hydroxide ion. *J. Chem. Soc., Dalton Trans.*, 845–849.

Oelkers E. H. (2001) General kinetic description of multioxide silicate mineral and glass dissolution. *Geochim. Cosmochim. Acta* **65**, 3703–3719.

Oelkers E. H. and Gislason S. R. (2001) The mechanism, rates and consequences of basaltic glass dissolution: I. An experimental study of the dissolution rates of basaltic glass as a function of aqueous Al, Si and oxalic acid concentration at 25 °C and pH 3 and 11. *Geochim. Cosmochim. Acta* **65**, 3671–3681.

Oelkers E. H. and Schott J. (1998) Does organic acid adsorption affect alkali feldspar dissolution rates? *Chem. Geol.* **151**, 235–245.

Oelkers E. H. and Schott J. (2009) Thermodynamics and kinetics of water-rock interaction. *Rev. Mineral. Geochem.* **70**, 569.

Oelkers E. H., Schott J. and Devidal J. L. (1994) The effect of aluminium, pH, and chemical affinity on the rates of aluminosilicate dissolution reactions. *Geochim. Cosmochim. Acta* **58**, 2011–2024.

Olsen A. A. and Rimstidt D. R. (2008) Oxalate-promoted forsterite dissolution at low pH. *Geochim. Cosmochim. Acta* **72**, 1758–1766.

Parruzot B., Jollivet P., Rébiscoul D. and Gin S. (2015) Long-term alteration of basaltic glass: mechanisms and rates. *Geochim. Cosmochim. Acta* **154**, 28–48.

Pelegrin E., Calas G., Ildefonse P., Jollivet P. and Galoisy L. (2010) Structural evolution of glass during alteration: application to nuclear waste glasses. *J. Non-cryst. Solids* **356**, 44–49.

Pierce E. M., Rodriguez E. A., Calligan L. J., Shaw W. J. and McGrail B. P. (2008) An experimental study of the dissolution rates of simulated aluminoborosilicate waste glasses as a function of pH and temperature under dilute conditions. *Appl. Geochem.* **23**, 2559–2573.

Rebiscoul D., Frugier P., Gin S. and Ayral A. (2005) Protective properties and dissolution ability of the gel formed during nuclear glass alteration. *J. Nucl. Mater.* **342**, 26-24.

Rosenberg D. R. and Maurice P. A. (2003) Siderophore adsorption to and dissolution of kaolinite at pH 3–7 and 22 °C. *Geochim. Cosmochim. Acta* **67**, 223–229.

Rozalen M., Ramos M. E., Huertas F. J., Fiore S. and Gervilla F. (2013) Dissolution kinetics and biodurability of tremolite particles in mimicked lung fluids. Effect of citrate and oxalate. *J. Asian Earth Sci.*, http://dx.doi.org/10.1016/j.jseas.2013.04.008.

Schalm O., Proost K., de Vis K., Cagno S., Janssens K., Mees F., Jacobs P. and Caen J. (2010) Manganese staining of archaeological glass: the characterization of Mn-rich inclusions in leached layers and a hypothesis of its formation. *Archaeometry* **53**, 103–122.

Shen S., Wu Z. and Peng W. (2014) Experimental study on weathering of seafloor volcanic glass by bacteria (*Pseudomonas fluorescens*) – implications for the contribution of bacteria to the water-rock reaction at the Mid-Oceanic Ridge setting. *J. Asian Earth Sci.* **90**, 15–25.

Silvestri A., Molin G. and Salviulo G. (2005) Archaeological glass alteration products in marine and land-based environments: morphological, chemical and microtextural characterization. *J. Non-cryst. Solids* **351**, 1338–1349.

Souza M. T., Crovace M. C., Schröder C., Eckert H., Peitl O. and Zanotto E. (2013) Effect of magnesium ion incorporation on the thermal stability, dissolution behavior and bioactivity in Bioglass-derived glasses. *J. Non-cryst. Solids* **382**, 57–65.

Staudigel H., Chastain R. A., Yayanos A. and Bourcier W. (1995) Biologically mediated dissolution of glass. *Chem. Geol.* **126**, 147–154.

Sterpenich J. (2011) Les interactions fluide/roche: des vitraux médiévaux à la sequestration géologique du CO_2. Thèse de doctorat, Université de Lorraine, 283p.

Stillings L. L., Drever J. I., Brantley S. L. and Sun Y. (1995) Rates of feldspars dissolution at pH 3–7 with 0–8 mM oxalic acid. *Chem. Geol.* **132**, 79–89.

Stillings L. L., Drever J. I. and Poulson S. R. (1998) Oxalate adsorption at a plagioclase (An47) surface and models for ligand-promoted dissolution. *Environ. Sci. Technol.* **32**, 2856–2864.

Stockmann G. J., Shirokova L. S., Pokrovsky O. S., Bénézeth P., Bovet N., Gislason S. R. and Oelkers E. H. (2012) Does the presence of heterotrophic bacterium *Pseudomonas reactans* affect basaltic glass dissolution rates? *Chem. Geol.* **296–297**, 1–18.

Stroncik N. A. and Schmincke H. U. (2002) Palagonite – a review. *Int. J. Earth Sci.* **91**, 680–697.

Techer I., Advocat T., Lancelot J. and Liotard J. M. (2000) Basaltic glass: alteration mechanisms and analogy with nuclear waste glasses. *J. Nucl. Mater.* **282**, 40–46.

Templeton D. (2002) *Molecular and Cellular Iron Transport*. CRC Press, 848 p.

Thien B. M. J., Gordon N., Ballestero A., Gin S. and Ayral A. (2012) The dual effect of Mg on the long-term alteration rate of AVM nuclear wase glasses. *J. Nucl. Mater.* **427**, 297–310.

Ullman W. J., Kirchman D. L., Welch S. A. and Vandevivere P. (1996) Laboratory evidence for microbially mediated silicate mineral dissolution in nature. *Chem. Geol.* **132**, 11–17.

Verney-Carron A., Gin S. and Libourel G. (2008) A fractured roman glass block altered for 1800 years in seawater: analogy with nuclear waste glass in a deep geological repository. *Geochim. Cosmochim. Acta* **72**, 5372–5385.

Wang X., Li Q., Hu H., Zhang T. and Zhou Y. (2005) Dissolution of kaolinite induced by citric, oxalic and malic acids. *J. Colloid Interface Sci.* **290**, 481–488.

Watkinson D., Weber L. and Anheuser K. (2005) Staining of archaeological glass from manganese-rich environments. *Archaeometry* **47**, 69–82.

Watteau F. and Berthelin J. (1994) Microbial dissolution of iron and aluminum from soil minerals: efficiency and specificity of hydroxamate siderophores compared to aliphatic acids. *Soil Biol.* **30**, 1–9.

Welch S. and Ullman W. (1992) The effect of organic acids on plagioclase dissolution rates and stoichiometry. *Geochim. Cosmochim. Acta* **57**, 2725–2736.

Welch S. A. and Ullman W. J. (1993) The effect of organic acids on feldspar dissolution rates and stoichiometry. *Geochim. Cosmochim. Acta* **57**, 2725–2736.

Wolff-Boenisch D. and Traina S. J. (2006) A comparative study of the effect of desferrioxamine B, oxalic acid, and Na-alginate on the desorption of U(VI) from goethite at pH 6 and 25 °C. *Geochim. Cosmochim. Acta* **70**, 4356–4366.

Wolff-Boenisch D. and Traina S. J. (2007) The effect of desferrioxamine B, enterobactin, oxalic acid, and Na-alginate on the dissolution of uranyl-treated goethite at pH 6 and 25 °C. *Chem. Geol.* **243**, 357–368.

Wolff-Boenisch D., Wenau S., Gislason S. R. and Oelkers E. H. (2011) Dissolution of basalts and peridotite in seawater, in the presence of ligands, and CO_2: implications for mineral sequestration of carbon dioxide. *Geochim. Cosmochim. Acta* **75**, 5510–5525.

Zinder B., Furrer G. and Stumm W. (1986) The coordination chemistry of weathering: II Dissolution of iron (III) oxides. *Geochim. Cosmochim. Acta* **50**, 1861–1869.

Associate editor: Lawrence M. Anovitz